Bimodal Distribution in the Fragmentation Behavior of Small Antimony Clusters Sb_x^+ ($x = 3–12$) Scattered from a Highly Oriented Pyrolitic Graphite Surface

Bernhard Kaiser,* Thorsten M. Bernhardt,† Bert Stegemann, Jörg Opitz, and Klaus Rademann
Walther-Nernst-Institut für Physikalische und Theoretische Chemie der Humboldt-Universität zu Berlin, Bunsenstrasse 1, D-10117 Berlin, Germany
(Received 23 February 1999)

The fragment ion-yield curves for the scattering of antimony cluster cations from highly oriented pyrolitic graphite show two clearly separated abundance maxima. On the low-energy side ($\leq 150 \pm 30$ eV) the interaction is characterized by the unimolecular fragmentation of the clusters and by neutralization as the competing process. The neutralization efficiency reaches a maximum at collision energies of 150 ± 30 eV. Above this boundary a transition to two different processes is indicated by a change in the fragment ion distribution. These competing processes are here the shattering and the implantation of the clusters. The threshold for implantation depends significantly on cluster size.

PACS numbers: 36.40.Qv, 34.50.–s, 61.46.+w, 68.55.Ln

Surfaces and interfaces play a very important role in applications such as catalysis and microelectronics. The controlled modification of these surfaces on a molecular level is therefore a challenging task in order to synthesize materials with new and unique properties. Mass selected clusters are very interesting in this respect, because their physical and chemical properties can be easily varied by a change of their size [1,2]. To prepare interfaces partially covered with clusters it is very important to understand the processes taking place during cluster surface interactions, which might lead to soft landing, neutralization, diffusion limited aggregation, fragmentation, sputtering, and implantation. All of these processes are known to be important, but detailed investigations on them are very rare [3–9]. Here we present data for the interaction of size-selected antimony cluster cations with highly oriented pyrolitic graphite (HOPG) over an extended energy range (0–600 eV) employing a new experimental setup, which combines the techniques of mass spectrometry and scanning tunneling microscopy (STM) for the elucidation of the underlying physical processes. In particular, we will show that unimolecular fragmentation and neutralization are the prevalent processes at low energy ($\leq 150 \pm 30$ eV), whereas shattering and implantation become predominant in the high-energy regime. The fragmentation behavior of the Sb_8^+ cluster ion will be discussed as representative for all investigated cluster sizes Sb_x^+ ($x = 3–12$).

The experimental setup consists of a three stage molecular beam apparatus coupled to a surface science setup via a scattering and deposition stage [10]. All parts have been designed to meet UHV requirements. Without operation of the molecular beam the base pressure of all chambers is below 10^{-10} mbar. Positively charged clusters are produced in a pulsed arc cluster ion source [11]. They are directed along the surface normal in a tandem time of flight mass spectrometer arrangement, which allows us to detect all positively charged collision products resulting from the surface impact. Prior to these studies the (0001)-basal plane of highly oriented pyrolitic graphite is cleaned by cleaving in air and heating to 600 °C in UHV for 60 minutes [12]. After the mass spectrometric investigations the surface is transferred to a modified BEETLE-type STM [13] without breaking vacuum.

Figure 1 shows fragment ion yield curves for the collision of Sb_8^+ with HOPG as a function of the mean collision energy. At low kinetic energies Sb_4^+ is the almost

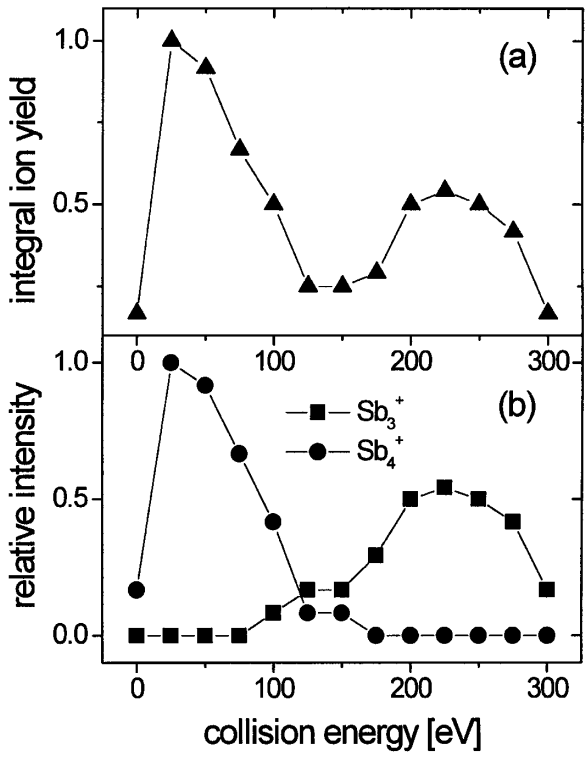

FIG. 1. (a) Integral ion yield and (b) relative intensity of the observed fragment ion peaks as a function of the mean collision energy for the scattering of Sb_8^+ from HOPG. The intensity of the Sb_4^+ fragment ion at 25 eV collision energy has been assigned as one.

 0031-9007/99/83(15)/2918(4)$15.00

exclusive fragment ion. Its intensity decreases with increasing collision energy and vanishes at energies greater than 150 eV. At energies around 100 eV a second fragment ion appears, the Sb_3^+. Its intensity reaches a maximum at 225 eV collision energy and then decreases down to zero at energies greater than 300 eV. The fragment ion yield shows a distinct minimum in the energy range between 125 and 150 eV.

To explain this behavior we first survey the low-energy regime (below the minimum at $\approx$150 eV). The most abundant fragment ion in this energy regime is Sb_4^+. This observation can be explained by the loss of a neutral Sb_4 cluster from the Sb_8^+ mother ion, which is in accordance with the special stability of the Sb_4 molecule. Its total binding energy amounts to 8.9 eV and its abundance in the vapor above solid antimony has been found to be greater than 90% [14,15]. Furthermore, using gas condensation techniques to produce antimony clusters only clusters containing a multiple of four atoms are observed [16]. With increasing kinetic energy the fragment ion distribution shifts from Sb_4^+ to the smaller cluster ion Sb_3^+. This is in agreement with a sequential unimolecular decay of the ions to form the most stable products according to the following reaction scheme:

$$Sb_8^+ \xrightarrow[E_{D,2}=1.3\ \mathrm{eV}]{-Sb_4} Sb_4^+ \xrightarrow[E_{D,3}=2.7\ \mathrm{eV}]{-Sb} Sb_3^+. \qquad (1)$$

The fragmentation channels given in the reaction sequence

$$Sb_3^+ \xrightarrow[E_{D,4}=4.2\ \mathrm{eV}]{-Sb} Sb_2^+ \xrightarrow[E_{D,5}=3.16\ \mathrm{eV}]{-Sb} Sb^+ \qquad (2)$$

have not been observed with high abundance (the dissociation energies have been taken from Refs. [14,17]). Instead the total fragment ion yield [Fig. 1(a)] decreases and reaches a minimum value at about 150 eV collision energy. It is well known that neutralization is an important process in the interaction of low-energy ions with a conducting surface [18–21]. So, we characterize the ion yield behavior in the low-energy regime (below 150 eV) by the occurrence of two competing processes: (i) sequential unimolecular fragmentation to form the most stable products and (ii) neutralization of the incoming particle.

The neutralization probability increases with increasing kinetic energy leading to almost 100% efficiency at a collision energy of about 150 eV. Such a behavior is in agreement with a resonant neutralization mechanism of the clusters and has also been observed for the interaction of atomic and molecular ions with different surfaces [22–24].

At higher collision energies the fragment ion yield increases again. In this high-energy regime Sb_3^+ is almost the only fragment ion observed. According to the reaction scheme (2) we would expect that at these high collision energies mainly the small fragment ions Sb_1^+, Sb_2^+, and Sb_3^+ should appear in the mass spectra. This poses several questions: (i) Why do we observe almost exclusively Sb_3^+? (ii) Why is the particle charged after the neutralization rate has reached almost 100% at 150 eV?

The fragmentation of the neutralized particle in this high-energy regime is not supposed to take place in a unimolecular decay pattern. Instead, the steep increase in internal cluster energy acquired very rapidly in the high-energy collision (collision time $<$ 100 fs) will more likely lead to a fast decomposition (shattering) of the clusters into small fragments [5,25]. A second process is then necessary to form the charged ions from the neutral fragments. Because the fragmentation happens in a very short time the neutral products are still on or very near to the surface. These neutrals may then leave the surface as ions with a certain probability P, which is given by the Saha-Langmuir equation:

$$P = \frac{q^+}{q} \exp\left(\frac{\Phi - IP}{k_B T}\right), \qquad (3)$$

where q and q^+ are the partition functions for the neutral and ionic cluster, Φ is the work function of the surface (5 eV for graphite [26]), IP is the ionization potential of the neutral cluster fragment, k_B is the Boltzmann constant, and T is the temperature of the cluster. Such a process has been observed previously for the interaction of anthracene molecules with a diamond surface [27]. From Eq. (3) we deduce that the probability for surface ionization favors the formation of Sb_3^+ (due to its exceptionally low IP compared to the next smaller and larger cluster sizes, $IP(Sb) = 8.6$ eV, $IP(Sb_2) = 8.4$ eV, $IP(Sb_3) = 6.61$ eV, $IP(Sb_4) = 7.56$ eV [28,29]), which is in agreement with the experimental observation of the almost exclusive abundance of the Sb_3^+ fragment. This model also suggests an increase in the Sb_3^+ fragment ion yield with increasing kinetic energy, and this is indeed observed. But then the intensity of the Sb_3^+ fragment ion reaches a maximum and decreases afterwards down to zero (cf. Fig. 1). In order to understand this trend, we investigated the surface by STM. At low collision energy (70 eV) only the flat graphite surface [Fig. 2(a)] is observed, whereas we find hillocks at high kinetic energies [230 eV, Fig. 2(b)]. These hillocks are very stable with time and are not influenced by the scanning motion of the tip. We attribute these nanodots to the implantation of the cluster into the surface: The impact leads to a very fast heating and subsequent cooling of the cluster and the surface atoms leaving a highly amorphous local spot at this surface site [30]. Counting the number of nanodots as a function of kinetic energy, we observe a clear threshold for their appearance (Fig. 3). The threshold correlates very well with the decrease in the Sb_3^+ fragment ion intensity and it depends significantly on cluster size. It is thus possible to directly relate the impact energy dependent decrease of scattering intensity to the process of surface implantation. Implantation has been observed for fullerenes and for silver clusters at high impact energies, too [9,31].

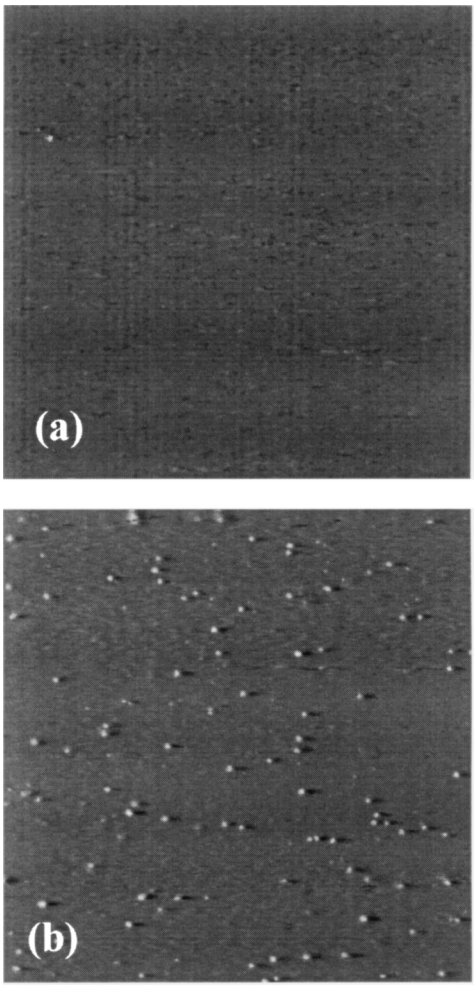

FIG. 2. 248 nm × 248 nm constant-current STM scan of the HOPG surface after irradiation with Sb_4^+ for one hour at (a) 70 eV kinetic energy (bias voltage $U_B = 500$ mV, tunnel current $I = 0.5$ nA) and (b) 230 eV kinetic energy ($U_B = 640$ mV, $I = 0.5$ nA). The average height of the nanodots in (b) is 4 Å.

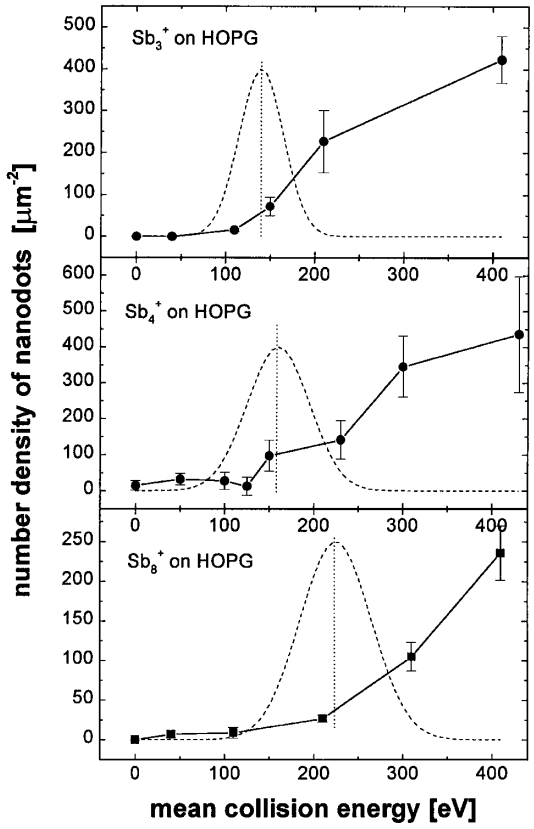

FIG. 3. The number of nanodots per surface area for three different cluster sizes as a function of mean collision energy. The straight line is drawn to guide the eye. The dashed line is a Gaussian fit to the measured intensity distribution of the Sb_3^+ fragment ion in the high-energy regime. The dotted line shows how the maximum in the Sb_3^+ fragment ion yield correlates with the onset of implantation (around 100 nanodots μm^{-2}).

Similar observations as we have just discussed for the Sb_8^+ cluster have been made for all investigated cluster sizes Sb_x^+ ($x = 3-12$). In summary we can separate the interaction of positively charged antimony clusters with HOPG in two distinct energy regimes according to the observed phenomena: (i) low collision energy $\leq 150 \pm 30$ eV: unimolecular fragmentation and neutralization; (ii) high collision energy $\geq 150 \pm 30$ eV: shattering and implantation.

The boundary between these regimes depends only weakly on cluster size, whereas the onset of implantation is significantly cluster size dependent. Each of these regimes offers a wealth of possibilities for the study of cluster properties and for the preparation of new materials with a controlled composition.

Financial support by the Deutsche Forschungsgemeinschaft, the Fonds der Chemischen Industrie, and the Humboldt-Forschungsfonds is gratefully acknowledged.

*Electronic address:
http://www.chemie.hu-berlin.de/sonst/bernd/index.html
†Present address: A. A. Noyes Laboratory, California Institute of Technology, Pasadena, CA 91125.

[1] A. W. Castleman, Jr. and K. H. Bowen, Jr., J. Phys. Chem. **100**, 12 911 (1996).
[2] *Clusters of Atoms and Molecules*, edited by H. Haberland (Springer, Berlin, 1994).
[3] H.-P. Cheng and U. Landman, J. Phys. Chem. **98**, 3527 (1994).
[4] G. Bräuchle, S. Richard-Schneider, D. Illig, R. D. Beck, H. Schreiber, and M. M. Kappes, Nucl. Instrum. Methods Phys. Res., Sect. B **112**, 105 (1996).
[5] R. D. Beck, J. Rockenberger, P. Weis, and M. M. Kappes, J. Chem. Phys. **104**, 3638 (1996).
[6] T. M. Bernhardt, B. Kaiser, and K. Rademann, Z. Phys. Chem. **195**, 273 (1996).
[7] T. M. Bernhardt, B. Kaiser, and K. Rademann, Z. Phys. D **40**, 327 (1997).
[8] C. Felix, G. Vandoni, C. Massobrio, R. Monot, J. Buttet, and W. Harbich, Phys. Rev. B **57**, 4048 (1998).
[9] S. J. Carroll, S. G. Hall, R. E. Palmer, and R. Smith, Phys. Rev. Lett. **81**, 3715 (1998).

[10] B. Kaiser, T. M. Bernhardt, and K. Rademann, Nucl. Instrum. Methods Phys. Res., Sect. B **125**, 223 (1997).
[11] G. Ganteför, H. R. Siekmann, H. O. Lutz, and K. H. Meiwes-Broer, Chem. Phys. Lett. **165**, 293 (1990).
[12] J. J. Metois, J. C. Heyraud, and Y. Takeda, Thin Solid Films **51**, 105 (1978).
[13] K. Besocke, Surf. Sci. **181**, 145 (1987).
[14] D. Rayane, P. Melinon, B. Tribollet, B. Cabaud, A. Hoareau, and M. Broyer, J. Chem. Phys. **91**, 3100 (1989).
[15] J. Mühlbach, P. Pfau, E. Recknagel, and K. Sattler, Surf. Sci. **106**, 18 (1981).
[16] K. Sattler, J. Mühlbach, and E. Recknagel, Phys. Rev. Lett. **45**, 821 (1980).
[17] B. Cabaud, A. Hoareau, P. Nounou, and R. Uzan, Int. J. Mass Spectrom. Ion Phys. **11**, 157 (1973).
[18] A. Amirav, Comments At. Mol. Phys. **24**, 187 (1990).
[19] H. Niehus, W. Heiland, and E. Taglauer, Surf. Sci. Rep. **17**, 213 (1993).
[20] *Low Energy Ion-Surface Interactions,* edited by J. W. Rabalais (Wiley & Sons, Chichester, 1994).
[21] P. Weis, J. Rockenberger, R. D. Beck, and M. M. Kappes, J. Chem. Phys. **104**, 3629 (1996).
[22] H. Akazawa and Y. Murata, J. Chem. Phys. **92**, 5551 (1990).
[23] S. A. Miller, D. E. Riederer, Jr., R. G. Cooks, W. R. Cho, H. W. Lee, and H. Kang, J. Phys. Chem. **98**, 245 (1994).
[24] R. Souda, Int. J. Mod. Phys. B **11**, 685 (1997).
[25] E. Hendell, U. Even, T. Raz, and R. D. Levine, Phys. Rev. Lett. **75**, 2670 (1995).
[26] *Handbook of Chemistry and Physics,* edited by D. R. Lide (CRC Press, Boca Raton, 1995).
[27] A. Danon and A. Amirav, J. Phys. Chem. **93**, 5549 (1989).
[28] G. DeMaria, J. Drowart, and M. G. Inghram, J. Chem. Phys. **31**, 1076 (1959).
[29] R. K. Yoo, B. Ruscic, and J. Berkowitz, J. Electron Spectrosc. Relat. Phenom. **66**, 39 (1993).
[30] B. Kaiser, T. M. Bernhardt, and K. Rademann, Appl. Phys. A **66**, S711 (1998).
[31] R. P. Webb, M. Kerford, M. Kappes, and G. Bräuchle, Nucl. Instrum. Methods Phys. Res., Sect. B **122**, 318 (1997).